Anat Embryol (2001) 203:109–119

ORIGINAL ARTICLE

Alida Amadeo · Barbara Ortino · Carolina Frassoni

Parvalbumin and GABA in the developing somatosensory thalamus of the rat: an immunocytochemical ultrastructural correlation

Accepted: 7 September 2000

Abstract The calcium binding protein parvalbumin (PV) is widely distributed in the mammalian nervous system and its relationship with GABAergic neurons differs within thalamic nuclei and animal species. In the rat somatosensory thalamus PV immunoreactive (ir) neurons were found only in the GABAergic reticular thalamic nucleus (RT), while a dense PVir neuropil is present in the ventrobasal complex (VB). In this study the distribution and relationship of PV and GABA were investigated in RT and VB during postnatal development at electron microscopic level. The pre-embedding immunoperoxidase detection of PV was combined with the post-embedding immunogold localization of GABA. In RT, at all developmental ages, neuronal cell bodies, dendrites and rare axonal terminals were both PVir and GABAir. In VB during the first postnatal week several small vesicle-containing profiles were double-labelled and some of them were identifiable as synaptic terminals. From postnatal day 7 (P7) to P9 the medial part of VB was more intensely PVir than the lateral one and some differences in the sequence of maturation of PVir terminals were noted between these two VB subdivisions. Single-labelled PVir profiles were first observed at P8, whereas single-labelled PVir terminals appeared at P12 and at P15 they became more frequent and larger, showing the typical morphology of ascending afferents described in adult VB. These results demonstrate the late expression of PV and acquisition of adult morphology in ascending terminals of rat VB during postnatal development in comparison with the innervation arising from the GABAergic RT.

A. Amadeo (✉), B. Ortino
Sezione di Istologia e Anatomia Umana,
Dipartimento di Fisiologia e Biochimica Generali,
Università degli Studi di Milano,
Via Celoria 26, 20133 Milano, Italy
e-mail: Alida.Amadeo@unimi.it
Tel.: +39-02-70644306, Fax: +39-02-2362808

C. Frassoni
Dipartimento di Neurofisiologia Sperimentale,
Istituto Neurologico “C. Besta”, Milano, Italy

Keywords Electron microscopy · Synapses · Development · Reticular thalamic nucleus · Ventrobasal complex

Introduction

Numerous studies have pointed out the importance of the differential and restricted distribution of the calcium binding proteins (CaBPs) parvalbumin (PV), calbindin and calretinin in the mammalian nervous system (Celio 1990; Résibois and Rogers 1992; Andressen et al. 1993). In particular, several lines of evidence have indicated that in thalamic nuclei these CaBPs are variously expressed in different mammalian species (Jones and Hendry 1989; Bentivoglio et al. 1990; Rausell et al. 1992; Arai et al. 1994; De Biasi et al. 1994a; Herron et al. 1997) and during development (Frassoni et al. 1991, 1998). In the adult rat thalamus PV is expressed only by neurons of the reticular nucleus (RT) and by axonal fibers and puncta in different nuclei of the dorsal thalamus (Celio 1990; Arai et al. 1994). During postnatal development a lateromedial gradient of the PV expression in the dorsal thalamus has been reported (Frassoni et al. 1991), so that at birth PV immunoreactivity is already evident in RT neurons and in fibers and puncta of the adjacent ventrobasal complex (VB), two of the thalamic nuclei involved in the processing of somatosensory inputs. On the contrary, the posterior thalamic nucleus, the third main somatosensory system-related thalamic nucleus, virtually lacks PV immunoreactivity at all developmental ages and in adulthood (Frassoni et al. 1991; Arai et al. 1994; Williams et al. 1994). In spite of the intense PV immunoreactivity described by light microscopy, no ultrastructural studies have so far been performed to characterize the PV-positive profiles in RT and VB.

As in other brain areas, the PV immunoreactive (ir) neurons of rat RT also contain the major inhibitory transmitter γ-aminobutyric acid (GABA; De Biasi et al. 1986, 1988; Arcelli et al. 1997). On the contrary, thalamic-projecting neurons in the brainstem are PV-positive but non-

GABAergic (Bennett-Clarke et al. 1992; Polgar and Antal 1995; Magnusson et al. 1996). As a consequence, in double-labelling experiments using antisera against PV and GABA in the somatosensory thalamus, the terminals originating from RT can be identified by their expression of both GABA and PV, whereas the terminals ascending from brainstem can be identified by their single PV immunoreactivity. Finally, the virtual absence of GABAergic local circuit neurons in rat VB (Barbaresi et al. 1986; De Biasi et al. 1988, 1997), allows us to infer that the single GABA-positive terminals in this area originate from extrathalamic sources (Parent et al. 1988; Rajakumar et al. 1994; Shammah-Lagnado et al. 1996; Wang et al. 1999).

The aim of this study was to provide further information on the development of the intrinsic synaptic circuitry of RT and VB by investigating and correlating at the electron microscopic level the expression of PV and GABA from birth to adulthood.

In particular, by combining PV and GABA ultrastructural immunolocalizations, we could identify the PVir GABA-negative lemniscal afferents to VB (Bennett-Clarke et al. 1992; Williams et al. 1994; Magnusson et al. 1996) and analyze their maturational sequence during postnatal development. Our results complement previous light microscopic studies on the development of ascending trigeminal afferents to the medial part of the rat VB (ventroposteromedial nucleus; VPM)(Huang 1989; Chiaia et al. 1991; Killackey 1993; Jacquin et al. 1996; Leamey and Ho 1998), and the scarce data available on the development of projections from the dorsal column nuclei (DCN; Asanuma et al. 1988; Spreafico et al. 1993; De Biasi et al. 1994b) to its lateral portion (ventroposterolateral nucleus; VPL).

Preliminary results have been presented in abstract form (Amadeo et al. 1997).

Materials and methods

Animals

The present study is based on rats (Wistar, Charles River Italia, Calco, LC, Italy) ranging from the day of birth, defined as postnatal day 0 (P0), to the end of the second postnatal week (P15) and adult animals. A total of 16 rats were studied as follows: P0, *n*=1; P4, *n*=2; P7, *n*=2; P8, *n*=1; P9, *n*=2; P12, *n*=3; P15, *n*=2; adult, *n*=3. All the experiments were undertaken in accordance with guidelines established in the Principles of Laboratory Animals Care (NIH Pubblication No. 86-23, revised 1985). All efforts were made to minimize animal suffering and to reduce the number of animals used. No in vitro alternatives were possible to obtain the results presented in the paper.

After anaesthesia with chloral hydrate (4%, 2 ml/100 g body weight) by intraperitoneal injection, the rats were perfused transcardially with a fixative solution containing 4% paraformaldehyde and 0.5% glutaraldehyde (fixative A) in 0.1 M phosphate buffer (PB), pH 7.2, after a rapid wash with 1% paraformaldehyde. Two animals (P8 and P12) were perfused with a different solution containing 2.5% glutaraldehyde and 0.5% paraformaldehyde (fixative B). Brains were then removed from the skull and postfixed in 4% paraformaldehyde. Serial, coronal sections (50–60 µm thick) were cut through the diencephalon using a Vibratome 1000 (Ted Pella, Redding, Calif.), collected in cold PB and used for PV immunolocalization. Alternate sections adjacent to those processed for immunocytochemistry were stained with thionin and the atlases of Paxinos et al. (1991) and Paxinos and Watson (1986) were used for the identification of developing and adult thalamic nuclei respectively.

Immunocytochemistry for PV

Serial, alternate sections throughout the whole rostrocaudal extent of RT were processed for the immunocytochemical detection of PV. After quenching of aldehyde groups with 0.05 M NH_4Cl in PB (30 min), sections were treated with 1% H_2O_2 (5 min) in PB to block endogenous peroxidases. The sections from rats perfused with high concentration of glutaraldehyde were also treated with 1% $NaBH_4$ in PB (15 min). The penetration of immunoreagents was increased by freezing the sections in liquid nitrogen and thawing in PB containing 20% sucrose, after cryoprotection in 10% and 20% PB-sucrose (1 h each). The pretreatment (30 min) with 10% normal goat serum (NGS) in phosphate buffered saline (PBS) was followed by incubation overnight at room temperature in a rabbit polyclonal antiserum raised against rat PV (SWant, Bellinzona, Switzerland) diluted 1:10,000 in PBS containing 1% NGS. The specificity characteristics of this antibody have been previously described (Celio 1990). After multiple rinses in PBS, sections were incubated for 75 min in biotinylated goat anti-rabbit IgG (Vector Laboratories, Burlingame, Calif.) diluted 1:200 in PBS/NGS 1%, rinsed in PBS, and incubated for 75 min in the avidin-biotin peroxidase complex (ABC kit, Vector, 1:100 in PBS/NGS 1%). After rinsing in PBS and in 0.05 M TRIS HCl buffer (pH 7.6) sections were reacted in a fresh solution containing 0.05% diaminobenzidine tetrahydrochloride (DAB; Sigma, Aldrich, Milano, Italy) and 0.002% H_2O_2 in TRIS HCl. Sections were then rinsed in buffer, mounted on gelatine-coated slides, dehydrated, and coverslipped. Substitution of the primary antiserum by preimmune serum and omission of the various steps in the immunocytochemical procedure resulted in no immunolabelling in control sections.

Electron microscopy

Some of the PV-immunolabelled sections containing RT and VB were selected from P4, P7, P8, P9, P12, P15, and adult brains. After postfixation with 2.5% glutaraldeyde (10 min) and then with 1% osmium tetroxide in PB (1 h), sections were dehydrated in ethanol and flat embedded in Epon-Spurr between acetate sheets (Aclar, Ted Pella, Redding, Calif.). Blocks were trimmed out under a dissection microscope from RT, VPL and VPM nuclei and glued to epoxy blanks. Thin sections were cut with a Reichert ultramicrotome and collected on nickel grids.

Fig. 1A–G Photomicrographs showing the distribution of PVir in the reticular nucleus (*RT*) and in the ventrobasal complex (*VB*) in coronal sections of the thalamus at different postnatal ages. **A** P0; the heavy labelled RT nucleus and PVir fibers (*arrowheads*) within VB. **B** P0; higher magnification of the PVir neuropil in VB. Several PVir terminal swellings and puncta (*arrows*) are scattered among parallel PVir fibers (*arrowheads*). **C** P7; beside the PVir neurons of RT the lateral portion of VB (*VPL*) shows a faint labelling as compared to the adjacent medial portion (*VPM*), where rods of PVir neuropil are evident (*arrowheads*). Some PVir cells (*arrows*) are scattered in VB. **D** P9; a peculiar arrangement of PVir is still present in VPM in comparison with the neuropil of VPL. **E** P9; detail of the dense network of PVir fibers in VPM. **F** P15; **G** Adult (*Ad*); from the end of the second postnatal week and in the adult thalamus, VB appears homogeneously innervated by PVir fibers. Ventrally the medial lemniscus (*arrowheads*) is also PVir. *Bars* 100 µm in A, C, D, F, G; 50 µm in B, E ▶

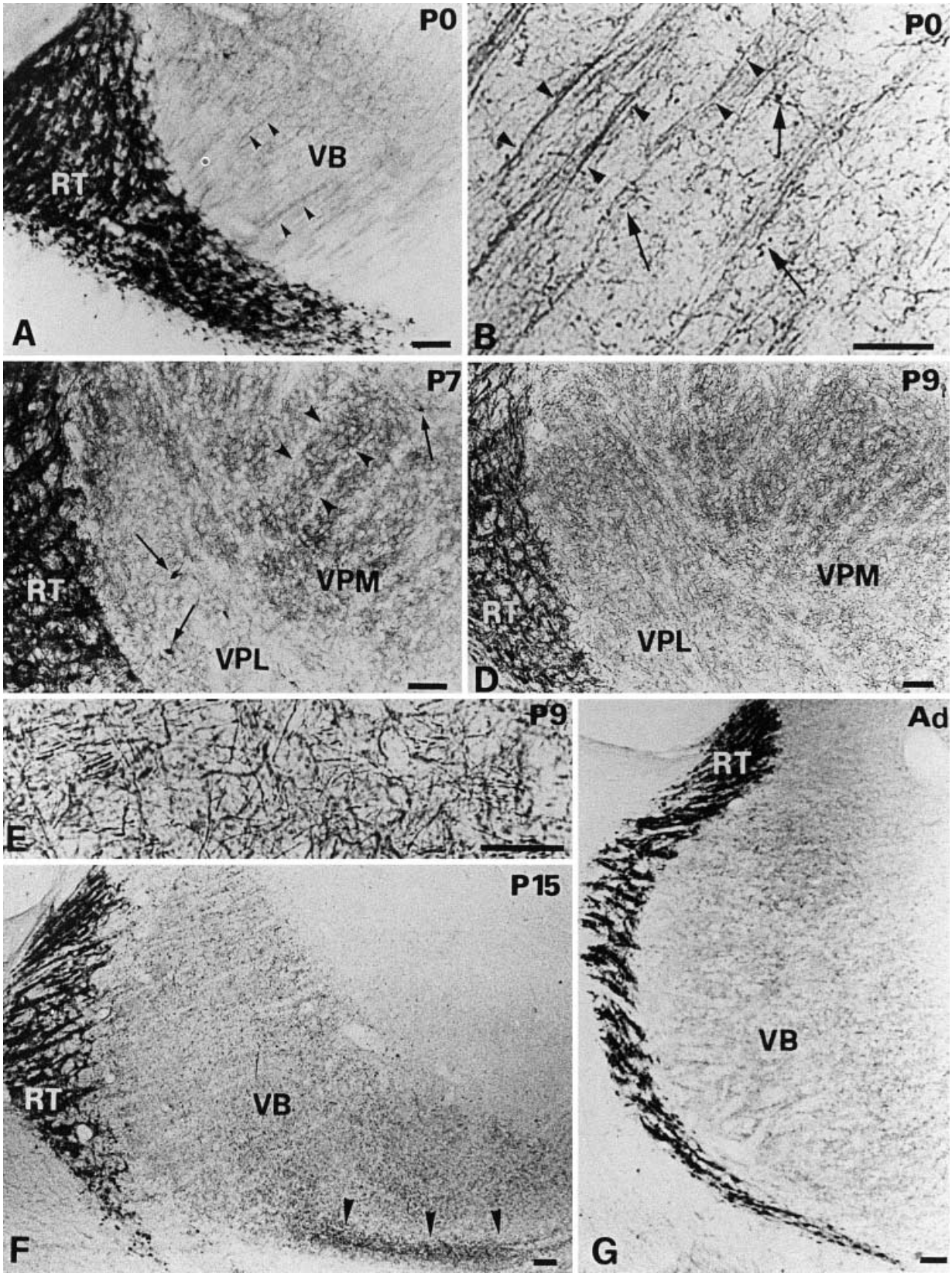
P0
RT
VB
A
P0
B
P7
RT
VPM
VPL
P9
RT
VPM
VPL
D
P9
E
Ad
RT
VB
P15
RT
VB
F
G

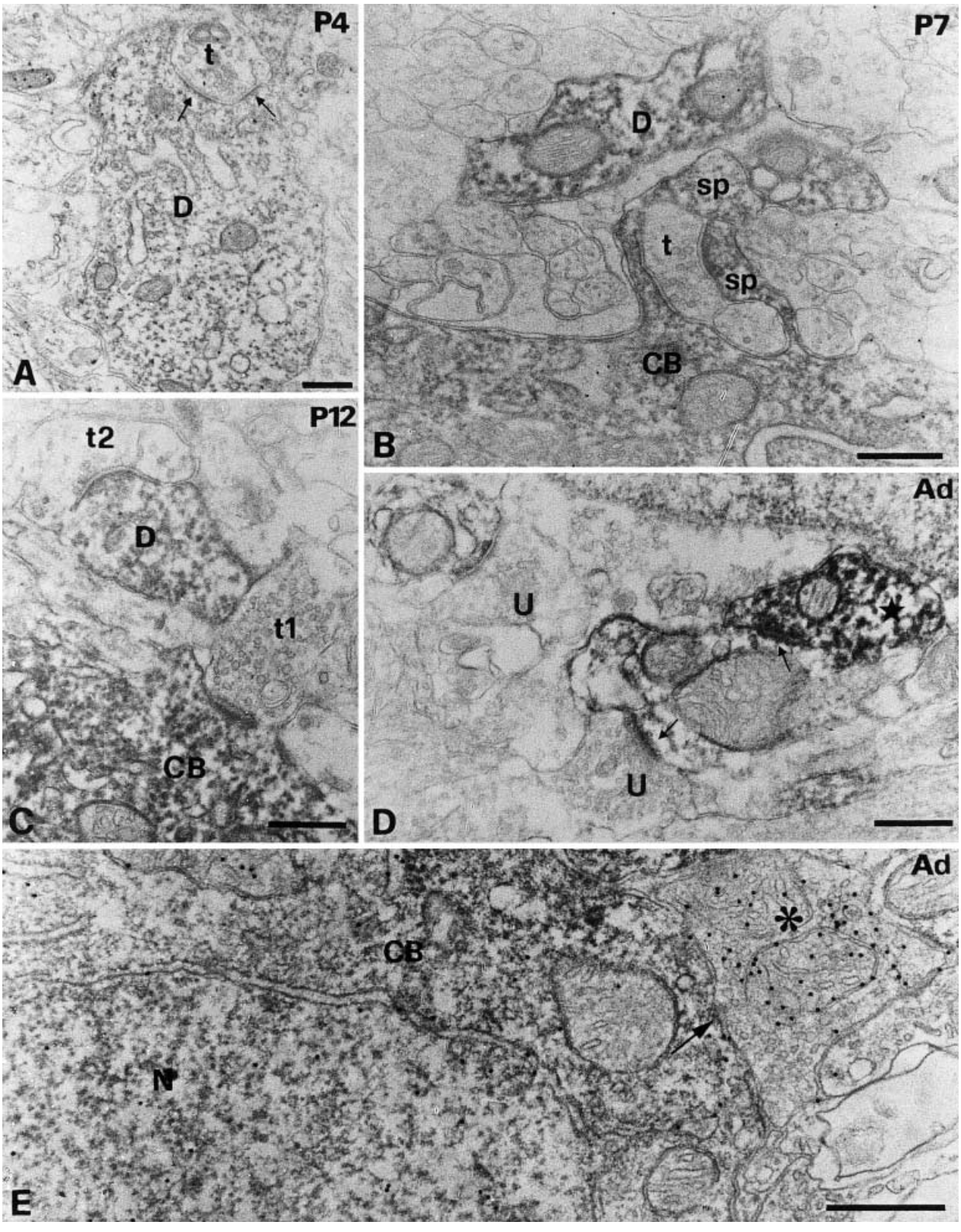

Fig. 2 Electron micrographs of PV (**A–E**) and GABA (**A, B, E**) immunolabelling in the developing and adult RT. **A** P4; a proximal double-labelled dendrite (*D*) is contacted by a small unlabelled terminal (*t*) showing two postsynaptic specializations (*arrows*). **B** P7; a small terminal (*t*) is surrounded by two somatic protrusions (*sp*) arising from a labelled cell body (*CB*) of RT (*D* labelled dendrite). **C** P12; a PVir cell body (*CB*) receives a synaptic contact by a terminal (*t1*) containing many round clear vesicles. Nearby an immature terminal (*t2*) forms a "frown" synapse with a distal PVir dendrite (*D*). **D** Adult (*Ad*); a PVir dendrite is contacted (*arrows*) by two boutons, one of which is PVir (*star*; *U* unlabelled terminals). **E** Adult (*Ad*); a GABAir terminal (*asterisk*) makes a synaptic contact of symmetric type (*arrow*) on a double-labelled cell body (*CB*; *N* nucleus). *Bars* 0.5 µm

Immunocytochemistry for GABA

To demonstrate the relationship between PVir and GABAir profiles, pre embedding immunoreaction for PV on some of the thin sections was combined with a post embedding immunogold procedure for the detection of GABA. For two selected and crucial postnatal ages (P8 and P12) the use of fixative B containing a high concentration of glutaraldehyde gave better results for GABA immunolabelling than fixative A.

After immersion in 0.5% aqueous sodium borohydride (5–8 min for postnatal tissue, 10 min for adults), grids were rinsed in 0.05 M TRIS buffered saline pH 7.6 (TBS), incubated at room temperature with 3% NGS (30 min) and then with the anti-GABA serum (Sigma, Aldrich, Milano, Italy; 1:10,000) in TBS (overnight at room temperature). After extensive rinses in TBS and TBS containing 0.2% bovine serum albumin (BSA), grids were incubated for 1 h at room temperature in a solution of goat anti-rabbit immunoglobulins coupled to 15 nm gold particles (Biocell, Cardiff, U.K.), diluted 1:20 in TBS (pH 8.2) containing 1% BSA. Several rinses in TBS and distilled water were followed by staining with lead citrate (2 min). Controls for GABA immunogold labelling were done on thin sections using the anti-GABA serum preadsorbed with GABA, as previously described in detail (De Biasi et al. 1994c), or by omitting the primary antiserum from the labelling sequence. No colloidal gold particles were seen in control sections.

Thin sections, with or without immunogold labelling, were counterstained or not with lead citrate, and examined with a Jeol T8 (Tokyo, Japan) electron microscope. The ultrastructural identification of neuronal profiles in neonatal samples was performed using the morphological criteria described by Vaughn (1989) and De Biasi et al. (1996). As for the adult, the data on RT ultrastructure were related to previous electron microscopic studies (Ohara and Lieberman 1985; De Biasi et al. 1988), whereas the identification in VB of large terminals as ascending projections and of medium sized boutons with flat vesicles as RT afferents was based on the results of published ultrastructural analyses (Peshansky et al. 1985; De Biasi et al. 1994c; Williams et al. 1994).

Results

Light microscopy

The examination of thalamic sections immunolabelled for PV at the different postnatal ages showed that RT neurons and VB neuropil were intensely labelled as early as P0 (Fig. 1A). RT neurons showed PV immunoreactivity throughout the rostrocaudal and dorsoventral extent of the nucleus (Fig. 1A, C, D, F, G). Some differences were observed only in the rostral pole of RT during the first postnatal week, where an inhomogeneous distribution of PVir neurons was revealed.

In the developing VB some variations in the distribution of PV immunoreactivity were observed. During the first postnatal week, PV immunolabelling was generally present in several parallel fibers arising from RT and following a lateromedial trajectory (Fig. 1A, B). Some of them showed terminal swellings morphologically similar to growth cones (Fig. 1B). Moreover, few scattered multipolar PVir neurons were observed in VPL (Fig. 1A, C) and rarely also in VPM (Fig. 1C). From the end of the first postnatal week VB appeared more intensely labelled than at previous ages and its two subdivisions (VPL and VPM) showed a different distribution of PV immunoreactivity (Fig. 1C). From P7 to P9 VPM appeared more intensely labelled than VPL and was characterized by peculiar clusters of PVir fibers and puncta (Fig. 1C–E) described also by Frassoni et al. (1991). From P9 the PVir innervation was homogeneously distributed in VPL and VPM (Fig. 1D, F, G). By the end of the second postnatal week also the medial lemniscus began to show PV immunoreactivity (Fig. 1F).

Electron microscopy

The ultrastructural analysis was performed on blocks containing RT, VPL and VPM at selected postnatal ages from P4 to P15 and in the adult. PV immunoreactivity could be visualized by the presence of DAB reaction product consisting of fine, granular electrondense material; in the double-labelled sections GABA immunoreactivity was easily distinguishable from PV immunoreactivity since it was represented by colloidal gold particles. The distribution of GABA-labelling in RT and VB of postnatal and adult rats was as previously reported (De Biasi et al. 1986, 1988, 1997), and therefore it will be described only in correlation with the distribution of PV immunoreactivity.

PV and GABA immunoreactivities in RT

During postnatal development PV immunoreactivity was detected in neuronal cell bodies, dendrites, growth cones and unmyelinated and (only from P8) myelinated fibers (Fig. 2A–E). PV-positive cell bodies often showed several somatic protrusions, sometimes surrounding unlabelled vesicle-containing profiles (Fig. 2B) or receiving presynaptically convex synaptic contacts from small terminals. In the adult RT few PVir axonal terminals contacting distal dendrites were found (Fig. 2D). In the double-labelled sections GABA immunoreactivity was present in most of the PV-positive structures (Fig. 2A, B, E); moreover an increasing number of single GABA-immunolabelled synaptic terminals was present from P4 to adult (Fig. 2E; see also De Biasi et al. 1997).

PV and GABA immunoreactivities in VB

In the two subdivisions of VB, VPL and VPM, PV immunoreactivity was generally found in axonal processes identifiable as growth cones, vesicle-rich profiles and synaptic terminals (Figs. 3A–F, 4A–E), whereas only very few dendritic profiles showed immunolabelling for PV. Since several modifications occurred in this region during postnatal development, the animals examined were divided into four age groups, also to better correlate PV and GABA immunoreactivities at the different developmental stages.

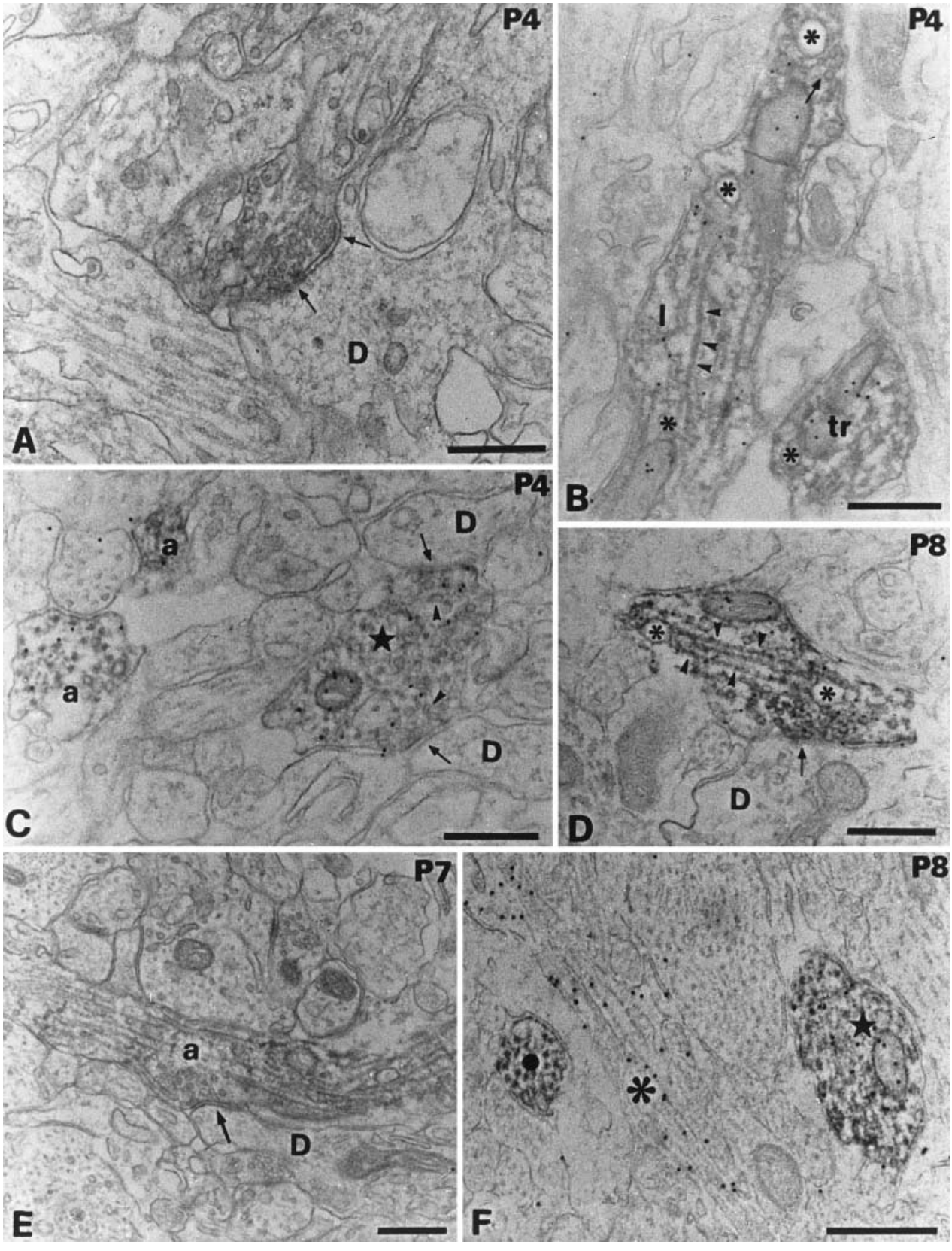
P4
D
A
P4
l
tr
B
P4
a
a
D
D
C
P8
D
D
P7
a
D
E
P8
F

P4–P7

During the first postnatal week PVir was present mainly in growth cones containing large vacuoles and microtubules, in irregular shaped vesicle-rich profiles and in small axons (Fig. 3B, E). Some small to medium sized PVir synaptic terminals were also observed (Fig. 3A, C, E); these boutons mostly contacted distal dendrites with synapses that were generally symmetric or undetermined and flat or "frown" (see De Biasi et al. 1996). In the double-labelling experiments GABA immunoreactivity was always present in all the described PV-positive profiles (Fig. 3B, C). At the end of the first postnatal week an increased number of double-labelled synaptic terminals was observed mainly in VPM.

P8–P9

At these ages most of medium-sized synaptic terminals (M type) were PVir and GABAir; they generally formed mature synapses of the symmetric type and contained small clear vesicles and mitochondria (Fig. 3D). Moreover, at this stage of postnatal development, besides double-labelled and single GABAir structures, an increasing number of single PVir small vesicle-rich profiles and axons was observed (Fig. 3F). In VPM they sometimes made synaptic contacts. Single PV immunoreactivity was rarely observed also in boutons making multiple synapses on different unlabelled profiles.

P12–P15

At P12 M type terminals were either single GABAir and double-labelled and they showed a mature morphology (Fig. 4A). The single PV-positive profiles were more frequent than in the previous developmental stage and larger than the double-labelled ones (Fig. 4B). These large PV-ir terminals (L type) were characterized by a pale immunolabelling and contained small clear vesicles, several dense core vesicles, mitochondria and bundles of microtubules (Fig. 4B); these terminals often made synapses of undetermined type on proximal dendrites and on several dendritic spines. In VPM the PV-positive L-type terminals were more frequently observed than in VPL. At P15 the distribution of PV and GABA immunoreactivities was very similar to that at P12; an increasing number of PVir L-type terminals, often very large and connected to the proximal dendrites by several puncta adhaerentia, was observed (Fig. 4C).

Adult

In the adult VB neuropil several types of synaptic terminals were morphologically and neurochemically recognized. Two different types of PVir boutons were characterized by their arrangement and morphology and by the presence or absence of GABA immunoreactivity. The L-type terminals were always GABA-negative and contacted proximal dendrites, more often on several dendritic spines, forming asymmetric synapses (Fig. 4D, E). The M-type terminals showed also GABA immunoreactivity and were generally more regular in shape and full of clear vesicles and mitochondria; they formed symmetric synapses with different targets including the proximal dendrites contacted by two or more L terminals (Fig. 4D). In the neuropil of VPM the PV-single labelled terminals were often smaller, still more frequent and clustered than in VPL (Fig. 4E).

Discussion

The present ultrastructural data demonstrate a different progressive maturation between the GABAergic system arising from RT and the ascending projections to VB. Some peculiar features of PV immunolabelling in RT and VB at certain stages of postnatal development will be commented upon and correlated with our ultrastructural analysis.

◀ **Fig. 3** Electron micrographs of PV (**A–F**) and GABA (**B, C, D, F**) immunoreactivities of the lateral (VPL) and medial (VPM) parts of VB of rats aged P4–P8. **A** P4, VPL; a PVir bouton containing round synaptic vesicles and cisterns of the smooth endoplasmic reticulum synapses (*arrows*) on an unlabelled dendrite (*D*). **B** P4, VPL; two double-labelled axonal growth cones, longitudinally (*l*) and trasversally (*tr*) sectioned, are rich in vacuoles (*asterisks*) and microtubules (*arrowheads*). A cluster of synaptic vesicles is present in one of them (*arrow*). **C** P4, VPM; two axonal profiles (*a*) and a synaptic terminal (*star*) are double-labelled. The terminal contains flat synaptic vesicles (*arrowheads*) and contacts (*arrows*) two different dendritic profiles (*D*). **D** P8, VPM; a bundle of microtubules (*arrowheads*) and two vacuoles (*asterisks*) are present in a double-labelled bouton contacting (*arrow*) a dendrite (*D*). **E** P7, VPL; a PVir axonal profile (*a*) makes an en passant symmetric synapse (*arrow*) with an unlabelled dendrite (*D*). **F** P8, VPL; axonal profiles in the neuropil are: double-labelled (*star*), single PVir (*dot*) and single GABAir (*asterisk*). *Bars* 0.5 µm

Fig. 4 Electron micrographs of PVir (**A–E**) and GABAir (**A, B, D**) structures in VB during the second postnatal week (**A–C**) and in the adult (**D, E**). **A, B** P12, VPL; several double-labelled vesicle containing profiles (*squares*) and an M type terminal (*star*) are present beside single GABAir processes (*triangles*), some single PVir structures (*dots*) and a single PVir large bouton (*asterisk*) containing bundles of microtubules (*arrowheads*), some dense core vesicles (*arrows*) and contacting different dendrites (*D*). **C** P15, VPM; a proximal dendrite (*D*) is contacted by a large PVir terminal (*asterisk*) with which it is connected by some puncta adhaerentia (*arrowheads*; *U* unlabelled terminal). **D** adult, VPL; a double-labelled M type terminal (*star*) makes a symmetric synapse (*arrow*) with a proximal dendrite (*D*) contacted on its spines (*s*) by a single PVir L-type bouton (*asterisk*). **E** adult, VPM; a cluster of PVir terminals of different sizes (*asterisks*) in the neuropil of VPM (*D* dendrites). *Bars* 0.5 µm ▶

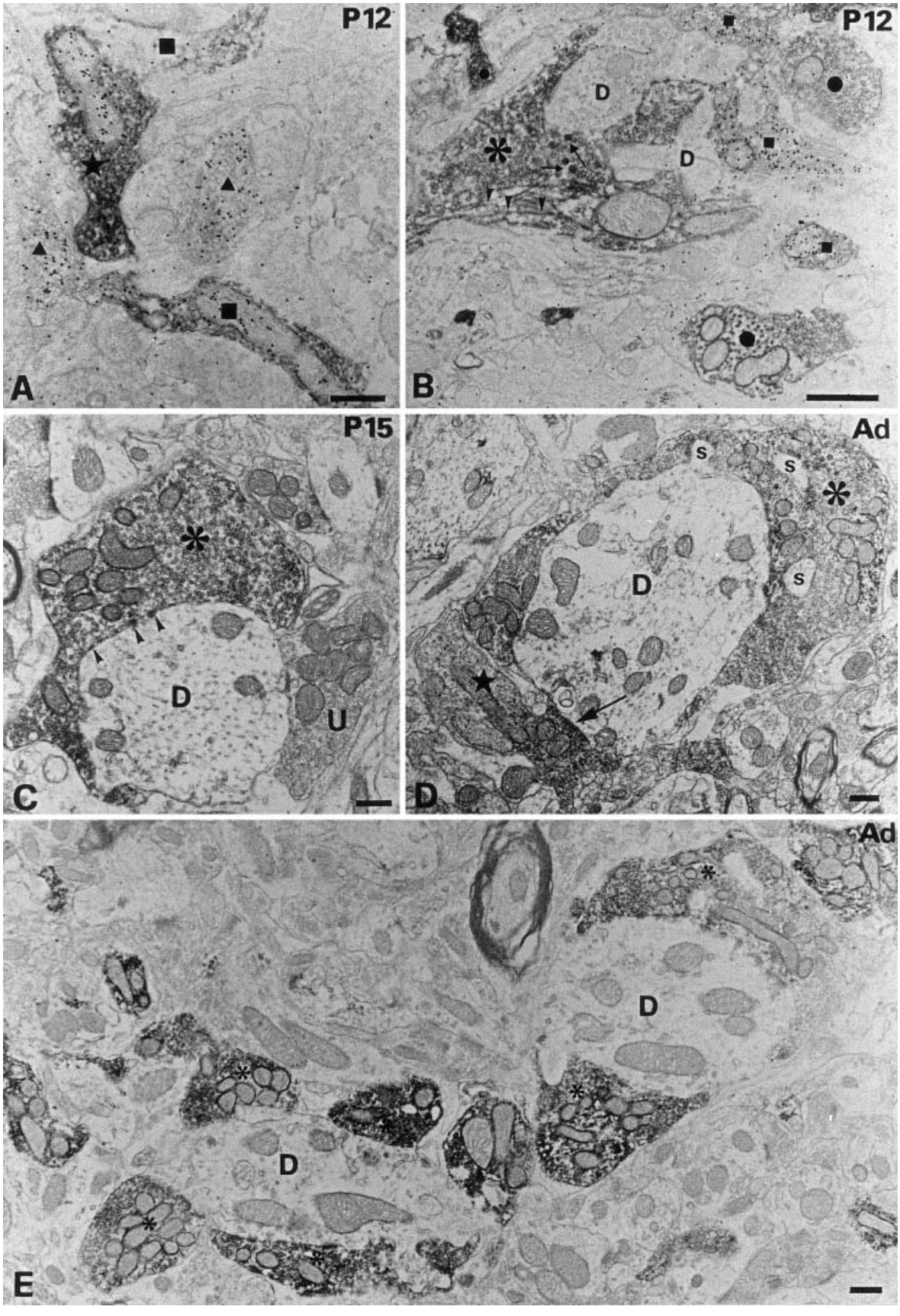

Fig. 4A–E

Reticular nucleus

PV and GABA are considered as markers of RT neurons during postnatal development and in the adult (De Biasi et al. 1986, 1997; Celio 1990; Frassoni et al. 1991; Mitrofanis 1992). An inhomogeneous distribution of PVir (this study; Mitrofanis 1992) and GABAir (A. Amadeo, personal communication) neurons was however observed in the rostral pole of RT at light microscopy, where a peculiar neurochemical content was also described in other studies (Arai et al. 1994; Lizier et al. 1997). As regards the somatosensory sector of RT, the ultrastructural finding of scarce PVir/GABAir terminals during development indicates that recurrent collaterals are rare in this area, thus confirming previous ultrastructural results (De Biasi et al. 1996; 1997). However, double-labelled terminals, representing recurrent collaterals, are also very few in adult RT (this study; Pinault et al. 1997), whereas the number of single GABA-positive terminals increases during development (De Biasi et al. 1996, 1997), suggesting that GABAergic terminals in RT mostly originate from extrathalamic sources (Asanuma and Porter 1990).

Ventrobasal complex

Our results show the presence of a few scattered PVir multipolar neurons with a restricted dendritic tree in the rat VB, presumedly representing the rare (less than 1%) GABAergic local circuit neurons of the rat VB (Harris and Hendrickson 1987; Arcelli et al. 1997).

The pattern of distribution of PVir neuropil in the rat VB confirms the previous study on PV expression in the rat thalamus during postnatal development (Frassoni et al. 1991), pointing out the increased PV immunoreactivity in VB and the transient hyperinnervation of its medial part (VPM) during the second postnatal week. In this study the sequential analysis of PV single expression and double PV/GABA immunolabelling in synaptic terminals of VB has been used as a tool to describe the development of some projections to this thalamic nucleus during the first two postnatal weeks. The PVir afferents to the adult rat VB originate essentially from: (a) the adjacent PVir and GABAir RT (Peschansky et al. 1983; De Biasi et al. 1988); (b) the trigeminal nucleus principalis (PrV) for VPM (Chiaia et al. 1991; Bennett-Clarke et al. 1992; Williams et al. 1994); (c) the DCN for VPL (Peshansky et al. 1985; Ma et al. 1987; De Biasi et al. 1994c; Magnusson et al. 1996). Among the PVir afferents to VB, those from RT are the most precocious, since RT neurons were shown to be already PVir at birth and to project to the thalamus during embryonic life (Solbach and Celio 1991; Mitrofanis and Baker 1993). Therefore it is likely that the PVir fibers with a lateromedial trajectory observed at light microscopy in the first postnatal days and the double-labelled boutons (M type) detected at electron microscopy in VB from P4 represent the reticulothalamic afferents characterized by morphological features that were consistent with a previous ultrastructural study (De Biasi et al. 1997). The expression of PV by ascending afferents from DCN and PrV was recently described in adults (Bennett-Clarke et al. 1992; Magnusson et al. 1996), yet scarce data are available on their development (Solbach and Celio 1991). Trigeminal afferents reach the thalamus at E17 (Leamey and Ho 1998), while lemniscal afferents do it in the first postnatal days (Asanuma et al. 1988). In this regard, recent studies have described the ultrastructural morphology of the afferents from DCN during early (P3) postnatal development by means of axonal tracing experiments (Spreafico et al. 1993; De Biasi et al. 1994b). However, in this study single PV immunoreactivity was never observed in VB neuropil during the first postnatal week, in line with preliminary data demonstrating the first appeareance of PVir neurons in DCN and PrV only from P8 on (S. De Biasi, unpublished observations). Just at this developmental stage (P8–9) the single PVir terminals (the future L type) began to be distinguished from the reticular double-labelled boutons (M type) exclusively for their different neurochemical content. Only at P12 single PVir terminals became larger, showing the typical features of ascending afferents (Ma et al. 1987; De Biasi et al. 1988, 1994c; Williams et al. 1994), in line with the findings of a recent ultrastructural study of the developing rat VB (De Biasi et al. 1996). On these bases, the increase of PV immunoreactivity observed in VB since the end of the first postnatal week could be due to the late expression of PV (second postnatal week) by the ascending afferents, which in turn can be correlated with the maturation of their physiological activity (Solbach and Celio 1991) and with the acquisition of a mature ultrastructural morphology that in the rat VB gradually develops by the second postnatal week (De Biasi et al. 1996, 1997).

The other interesting observation is that in VPM, during the second postnatal week, there is a transient PVir hyperinnervation and a peculiar distribution of PVir fibres that reflects the presence of rods of neural tissue, the barreloids, representing faithfully the vibrissae on the face (Killackey 1993; Land et al. 1995). In the rat VPM the barreloids are particularly evident during the first two postnatal weeks both with histochemical and axonal transport methods (Killackey 1993; Land et al. 1995), whereas after P15 they are obscured by a postnatal rotation of the rat VB relative to the major axes of the diencephalon (Land and Simmons 1985; Land et al. 1995). In line with these data, we could not identify PVir barreloids in the adult VB. The transient PVir hyperinnervation of VPM with respect to VPL during the second postnatal week could be explained by the particular concentration of reticular and trigeminal afferents in the core of barreloids that, rotating by P15 (Land et al. 1995), give rise to an apparent decrease of PV immunoreactivity in VPM. Alternatively, an overgrowth of ascending trigeminal afferents could be proposed (Asanuma et al. 1988).

At the ultrastructural level a slight difference between the maturational sequences of terminals in VPL and VPM was observed. During the first postnatal week the

PVir/GABAir synaptic terminals originating from RT are more easily found in VPM than in VPL, where they are generally smaller. Later, in the second postnatal week, the L-type terminals displaying single PV immunoreactivity appear larger, more mature and clustered in VPM than that in VPL. By contrast, in the adult VPM they were smaller but more numerous than in VPL. So far, no comparative data are available on the ultrastructural developmental features of VPL and VPM. However, an earlier arrival of afferents to VPM as compared with VPL has been reported (Asanuma et al. 1988; Killackey 1993; Spreafico et al. 1993; De Biasi et al. 1994b; Leamey and Ho 1998). On these bases, considering the precocious morphological maturity of PVir L-type terminals in the rat VPM and the correlation of PV expression with the stage of maturation of a particular afferent system (Solbach and Celio 1991), it could be suggested that in VPM the synaptic circuit organization develops slightly before that in VPL.

Finally, in the adult rat VB we clearly demonstrated the presence of two PVir afferent systems characterized by means of their neurochemical content and of their morphological features. Double-labelled reticular terminals (M type) showed the ultrastructural characteristics of the "F" boutons in the rat VB (De Biasi et al. 1988, 1994c), whose symmetric synapses and GABA content demonstrate their inhibitory function and their origin from RT. The large (L type) PVir synaptic terminals resemble the ascending afferents described in several axonal tracing studies both in VPL (Ma et al. 1987; De Biasi et al. 1988, 1994) and in VPM (Williams et al. 1994); however this study represents the first report of their PV immunoreactivity. These large PVir terminals contact mainly proximal dendrites and their spines both in VPL and in VPM. The only difference from the previous studies is the rarity of somatic PVir contacts that were described both for terminals arising from DCN (Ma et al. 1987; De Biasi et al. 1988) and from trigeminal afferents (Williams et al. 1994). Since PVir neurons projecting from brainstem to VB represent a subpopulation of the total neuronal group innervating the ventrobasal thalamus (Bennett-Clarke et al. 1992; Magnusson et al. 1996), it is possible that their terminals have a particular and more selected distribution on thalamic neurons. Furthermore, our observations demonstrate that the PVir L terminals in the adult are smaller, more numerous and clustered in VPM than in VPL. On these bases it could be suggested that the PVir trigeminal projections show a peculiar and more definite distribution and organization in the VPM neuropil in comparison with other ascending afferents to VB. This conclusion together with the early maturation of the trigeminal system could be correlated with the precise topographical organization of this sensory pathway.

Acknowledgements The authors are grateful to Prof. Silvia De Biasi and Prof. Roberto Spreafico for their suggestions and helpful comments on the manuscript. This work was supported by Ministero dell'Università e della Ricerca Scientifica e Tecnologica (MURST 60%) and Ministero della Sanità (MINSAN; Ricerca corrente).

References

Amadeo A, De Biasi S, Ortino B, Frassoni C, Spreafico R (1997) Parvalbumin immunoreactivity in the somatosensory thalamus: an electron microscopic correlation with GABA immunoreactivity in the developing and adult rat. Trends Neurosci [Suppl] 20: 53

Andressen C, Blumke I, Celio MR (1993) Calcium-binding proteins: selective markers of nerve cells. Cell Tissue Res 271: 181–208

Arai R, Jacobowitz DM, Deura S (1994) Distribution of calretinin, calbindin-D28k and parvalbumin in the rat thalamus. Brain Res 33: 595–614

Arcelli P, Frassoni C, Regondi MC, De Biasi S, Spreafico R (1997) GABAergic neurons in mammalian thalamus: a marker of thalamic complexity? Brain Res Bull 42: 27–37

Asanuma C, Porter LL (1990) Light and electron microscopic evidence for a GABAergic projection from the caudal basal forebrain to the thalamic reticular nucleus in rats. J Comp Neurol 302: 159–172

Asanuma C, Ohkawa R, Stanfield BB, Cowan WM (1988) Observations on the development of certain ascending inputs to the thalamus in rats. I. Postnatal development. Brain Res Dev Brain Res 41: 159–170

Barbaresi P, Spreafico R, Frassoni C, Rustioni A (1986) GABAergic neurons are present in the dorsal column nuclei but not in the ventroposterior complex of rat. Brain Res 282: 305–326

Bennett-Clarke CA, Chiaia NL, Jacquin MF, Rhoades RW (1992) Parvalbumin and calbindin immunocytochemistry reveal functionally distinct cell groups and vibrissa-related patterns in the trigeminal brainstem complex of adult rat. J Comp Neurol 320: 323–338

Bentivoglio M, Macchi G, Spreafico R, Frassoni C (1990) Calbindin and parvalbumin immunoreactivity in the feline thalamus. Eur J Neurosci S3: 275

Celio MR (1990) Calbindin D-28 k and parvalbumin in the rat nervous system. Neuroscience 35: 375–475

Chiaia NL, Rhoades RW, Bennett-Clarke CA, Fish SE, Killackey HP (1991) Thalamic processing of vibrissal information in the rat. I. Afferent input to the medial ventral posterior and posterior nuclei. J Comp Neurol 314: 201–216

De Biasi S, Frassoni C, Spreafico R (1986) GABA immunoreactivity in the thalamic reticular nucleus of the rat. A light and electron microscopical study. Brain Res 399: 143–147

De Biasi S, Frassoni C, Spreafico R (1988) The intrinsic organization of the ventroposterolateral (VPL) nucleus and related reticular thalamic nucleus (RTN) of the rat. A double labelling ultrastructural investigation with GABA immunogold staining and lectin-conjugated horseradish peroxidase (WGA-HRP). Somatosens Res 5: 187–204

De Biasi S, Arcelli P, Spreafico R (1994a) Parvalbumin immunoreactivity in the thalamus of guinea pig: light and electron microscopic correlation with gamma-aminobutyric acid immunoreactivity. J Comp Neurol. 348: 556–569

De Biasi S, Amadeo A, Arcelli P, Frassoni C, Spreafico R (1994b) Ultrastructural characterization of afferent terminals in the thalamic ventrobasal complex of neonatal rats. Eur J Neurosci S7: 162

De Biasi S, Amadeo A, Spreafico R, Rustioni A (1994c) Enrichment of glutamate immunoreactivity in lemniscal terminals in the ventropostero lateral thalamic nucleus of the rat: an immunogold and WGA-HRP study. Anat Record 240: 131–140

De Biasi S, Amadeo A, Arcelli P, Frassoni C, Meroni A, Spreafico R (1996) Ultrastructural characterization of postnatal development of the thalamic ventrobasal and reticular nuclei in the rat. Anat Embryol 193: 341–353

De Biasi S, Amadeo A, Arcelli P, Frassoni C, Spreafico R (1997) Postnatal development of GABA immunoreactive terminals in the reticular and ventrobasal nuclei of the rat thalamus: a light and electron microscopical study. Neuroscience 76: 503–516

Frassoni C, Bentivoglio M, Spreafico R, Sanchez MP, Puelles L, Fairen A (1991) Postnatal development of calbindin and parvalbumin immunoreactivity in the thalamus of the rat. Brain Res Dev Brain Res 58: 243–249

Frassoni C, Arcelli P, Selvaggio M, Spreafico R (1998) Calretinin immunoreactivity in the developing thalamus of the rat: a marker of early generated thalamic cells. Neuroscience 83: 1203–1214

Harris RM, Hendrickson AE (1987) Local circuit neurons in the rat ventrobasal thalamus: a GABA immunocytochemical study. Neuroscience 21: 229–236.

Herron P, Baskerville KA, Chang HT, Doetsch GS (1997) Distribution of neurons immunoreactive for parvalbumin and calbindin in the somatosensory thalamus of the racoon. J Comp Neurol. 388: 120–129

Huang LM (1989) Origin of thalamically projecting somatosensory relay neurons in the immature rat. Brain Res 495: 108–114

Jacquin MF, Rana JZ, Miller MW, Chiaia NL, Rhoades RW (1996) Development of trigeminal nucleus principalis in the rat: effects of target removal at birth. Eur J Neurosci 8: 1641–1657

Jones EG, Hendry SHC (1989) Differential calcium binding proteins immunoreactivity distinguishes classes of relay neurons in monkey thalamic nuclei. Eur J Neurosci 1: 22–246

Killackey HP (1993) The development of trigeminothalamic projections. In: Minciacchi D, Molinari M, Macchi G, Jones EG (eds) Thalamic networks for relay and modulation. Pergamon Press, Oxford, pp 39–48

Land PW, Simmons DJ (1985) Metabolic and structural correlates of the vibrissae representation in the thalamus of the adult rat. Neurosci Lett 60: 319–324

Land PW, Buffer SA, JR, Yaskosky JD (1995) Barreloids in adult rat thalamus: three-dimensional architecture and relationship to somatosensory cortical barrels. J Comp Neurol 355: 573–588

Leamey CA, Ho SM (1998) Afferent arrival and onset of functional activity in the trigeminothalamic pathway of the rat. Brain Res Dev Brain Res 105: 195–207

Lizier C, Spreafico R, Battaglia G (1997) Calretinin in the thalamic reticular nucleus of the rat: distribution and relationship with ipsilateral and contralateral efferents. J Comp Neurol 377: 217–233

Ma W, Peschanski M, Ralston III HJ (1987) The differential synaptic organization of the spinal and lemniscal projections to the ventrobasal complex of the rat thalamus. Evidence for convergence of the two systems upon single thalamic neurons. Neuroscience 22: 925–934

Magnusson A, Dahlfors G, Blomqvist A (1996) Differential distribution of calcium-binding proteins in the dorsal column nuclei of rats: a combined immunohistochemical and retrograde tract tracing study. Neuroscience 73: 497–508

Mitrofanis J (1992) Patterns of antigenic expression in the thalamic reticular nucleus of developing rats. J Comp Neurol 320: 161–181

Mitrofanis J, Baker GE (1993) Development of the thalamic reticular and perireticular nuclei in rats and their relationship to the course of growing corticofugal and corticopetal axons. J Comp Neurol 388: 575–587

Ohara PT, Lieberman AR (1985) The thalamic reticular nucleus of the adult rat: experimental anatomical studies. J Neurocytol 14: 365–411

Parent A, Paré D, Smith Y, Steriade M (1988) Basal forebrain cholinergic and noncholinergic projections to the thalamus and brainstem in cats and monkeys. J Comp Neurol 277: 281–301

Paxinos G, Watson C (1986) The rat brain in stereotaxic coordinates. Academic Press, New York

Paxinos G, Tork I, Tecott LH, Valentino KL (1991) Atlas of the developing rat brain. Academic Press, New York

Peschanski M, Ralston HJ III, Roudier F (1983) Reticularis thalami afferents to the ventrobasal complex of the rat thalamus: an electron microscope study. Brain Res 270: 325–329

Peschanski M, Roudier F, Ralston HJ III, Besson JM (1985) Ultrastructural analysis of the terminals of various somatosensory pathways in the ventrobasal complex of the rat thalamus: an electron-microscopic study using wheat-germ agglutinin conjugated to horseradish peroxidase as an axonal tracer. Somatosens Res 3: 75–87

Pinault D, Smith Y, Deschenes M (1997) Dendrodendritic and axoaxonic synapses in the thalamic reticular nucleus of the adult rat. J Neurosci 17: 3215–3233

Polgar E, Antal M (1995) The colocalization of parvalbumin and calbindin D28k with GABA in the subnucleus caudalis of the rat soinal trigeminal nucleus. Exp Brain Res 103: 402–408

Rajakumar N, Elisevich K, Flumerfelt BA (1994) Parvalbumin-containing GABAergic neurons in the basal ganglia output system of the rat. J Comp Neurol 350: 324–335

Rausell E, Bae CS, Vinuela A, Huntley GW, Jones EG (1992) Calbindin and parvalbumin cells in monkey VPL thalamic nucleus: distribution, laminar cortical projections, and relations to spino thalamic terminations. J Neurosci 12: 4048–4111

Résibois A, Rogers JH (1992) Calretinin in rat brain: an immunohistochemical study. Neuroscience 46: 101–134

Shammah-Lagnado SJ, Alheid GF, Heimer L (1996) Efferent connections of the caudal part of the globus pallidus in the rat. J Comp Neurol 376: 489–507

Solbach S, Celio MR (1991) Ontogeny of the calcium-binding protein parvalbumin in the rat nervous system. Anat Embryol 184: 103–124

Spreafico R, Frassoni, Regondi MC, Amadeo A, De Biasi S (1993) Morphological study on the postnatal development of rat somatosensory thalamus. Soc Neurosci Abstr 19: 45

Vaughn J (1989) Fine structure of synaptogenesis in the vertebrate central nervous system. Synapse 3: 255–285

Wang B, Gonzalo-Ruiz A, Sanz JM, Campbell G, Lieberman AR (1999) Immunoelectron microscopic study of gamma-aminobutyric acid inputs to identified thalamocortical projection neurons in the anterior thalamus of the rat. Exp Brain Res 126: 369–382

Williams MN, Zahm DS, Jacquin MF (1994) Differential foci and synaptic organization of the principal and spinal trigeminal projections to the thalamus in the rat. Eur J Neurosci 6: 429–453